

22. T. T. Perkins, S. R. Quake, D. E. Smith, S. Chu, unpublished results.
23. G. Ryskin, *J. Fluid Mech.* **178**, 423 (1987).
24. S. W. Provencher, *Comput. Phys. Commun.* **27**, 213 (1982).
25. The symmetry of the tethered chain yields only the odd modes within these models. The amplitudes for the Zimm model are approximate and are given in B. H. Zimm, G. M. Roe, L. F. Epstein, *J. Chem. Phys.* **24**, 279 (1956). The values reported are the average of the two solutions from the inverse Laplace transform. The ratios for the solution chosen by Provencher's algorithm were  $10.1 \pm 4.0$  for the times and  $2.3 \pm 0.9$  for the amplitudes. The corresponding values in the limit of small regularization are  $6.4 \pm 2.0$  and  $1.7 \pm 0.7$ .
26. P. G. de Gennes, *J. Chem. Phys.* **60**, 5030 (1974).
27. W. H. Press *et al.*, *Numerical Recipes* (Cambridge Univ. Press, Cambridge, 1989), pp. 309–317.
28. We acknowledge the generous assistance of J. Spudich and his colleagues, J. Finer, H. Goodson, and G. Nuckolls, including support through National Institutes of Health grant 33289 to J. Spudich. We also acknowledge the introduction to biochemistry given to S.C. by S. Kron, discussions with G. Fuller, R. Larson, R. Pecora, Y. Rabin, R. Stinchcombe, and B. Zimm, and the computer code and advice of S. Provencher. This work was supported in part by grants from the U.S. Air Force Office of Scientific Research and the National Science Foundation and by an endowment established by Theodore and Frances Geballe.

29 December 1993; accepted 1 April 1994

## Surface Vibrational Spectroscopic Studies of Hydrogen Bonding and Hydrophobicity

Quan Du, Eric Freysz,\* Y. Ron Shen†

Surface vibrational spectroscopy by sum-frequency generation was used to study hydrophobicity at the molecular level at various interfaces: water–surfactant-coated quartz, water–hexane, and water–air. In all cases, hydrophobicity was characterized by the appearance of dangling hydroxyl bonds on 25 percent of the surface water molecules. At the water–quartz interface, packing restrictions force the water surface layer to have a more ordered, ice-like structure. A partly wettable water–quartz interface was also studied.

Knowledge about interfacial water structure near hydrophobic surfaces is crucial for the understanding of many important surface problems involving water. For instance, wetting or nonwetting is a familiar phenomenon, but there is not yet a clear physical picture of the phenomenon at the molecular level (1). Hydrophobic interactions are responsible for the formation of micelles (2) and play an important role in organizing constituent molecules of living matter into complex structures such as membranes (2, 3). The understanding of hydrophobic interfaces can also provide a better picture of how hydrophobic solute particles are surrounded by water molecules when immersed in water (4). In the past, the importance of such interfaces has stimulated a number of theoretical studies done with numerical calculations (5–7). Experimental research on the topic, however, has been rare or nonexistent because of a lack of suitable techniques. Recently, infrared-visible sum-frequency generation (SFG) has been developed into a versatile surface spectroscopic tool that can be used to probe all types of interfaces, including liquid-liquid and solid-liquid interfaces (8–10).

Department of Physics, University of California, and Materials Sciences Division, Lawrence Berkeley Laboratory, Berkeley, CA 94720, USA.

\*Present address: Centre de Physique Moléculaire, Université de Bordeaux 1, 351 Avenue de la Libération, 33405 Talence CEDEX, France.

†To whom correspondence should be addressed.

We report vibrational spectroscopic measurements made on two hydrophobic interfaces. One was a water–solid interface, where the solid surface was rendered hydrophobic by a monolayer coating of surfactant OTS [octadecyltrichlorosilane,  $\text{CH}_3(\text{CH}_2)_{17}\text{SiCl}_3$ ], and the other was a water–hexane interface. The spectra were compared with that of the water–air interface, which can also be regarded as hydrophobic. In all cases, the hydrophobic interaction was characterized by the appearance of a free hydroxyl (OH) stretch peak of

water in the spectra. The bonded OH spectra of water at the different interfaces showed some clear differences, which suggested a difference in the water's interfacial structure. The water molecules against the solid wall appeared to be more bond-ordered. We also probed a partly wettable surface prepared by a monolayer coating of surfactants that had loosely packed hydrocarbon chains. No free OH peak was observed in that case.

The SFG technique has been described previously (8). Within the electric dipole approximation, the process is forbidden in a centrosymmetric bulk medium such as water but allowed at the surface, where the inversion symmetry is broken. For water interfaces, it has been shown (9) that the quadrupolar contribution from the bulk water is not appreciable and that the SFG in reflection comes mainly from the dipolar contribution of interfacial water molecules with preferred polar orientations.

The experimental setup for our SFG measurement has also been described elsewhere (8, 11). The hydrophobic solid surface was prepared by depositing a monolayer of OTS on the surface of a fused quartz window by means of a standard self-assembly technique (12). The hydrophobicity of the surface came from the layer of closely packed hydrocarbon chains. The SFG spectrum in the OH stretch region that was obtained from this quartz–OTS–water interface is shown in Fig. 1A. The sum-frequency (SF) output, visible input, and infrared (IR) input were s-, s-, and p-polarized, respectively (denoted by ssp). The results were similar to those obtained from an air–water interface (9), the ssp spectrum of which is shown in Fig. 1B for comparison. In both cases, the spectrum exhibited a sharp peak at  $3680 \text{ cm}^{-1}$  that can be assigned to the non-hydrogen-bonded OH

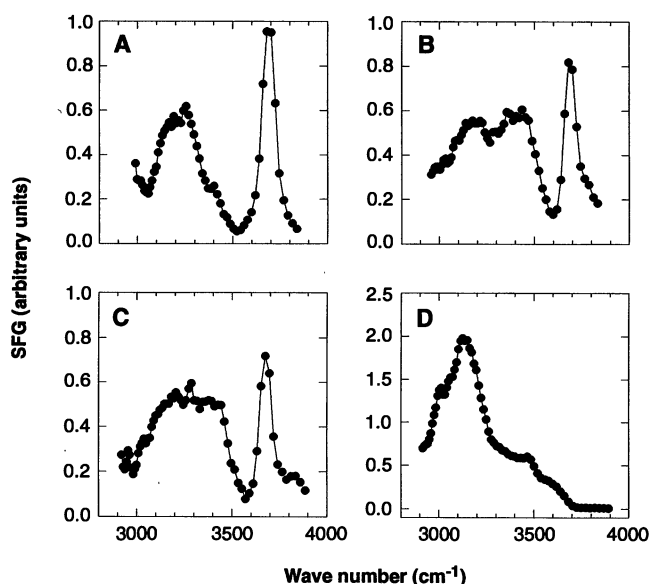


**Fig. 1.** SFG spectra from (A) the quartz–OTS–water interface, (B) the air–water interface, (C) the hexane–water interface, and (D) the quartz–ice interface. The SF output, visible input, and IR input were s-, s-, and p-polarized, respectively.

(free OH) stretch vibration (9). The broad spectral features between 3000 and 3600  $\text{cm}^{-1}$  were due to hydrogen-bonded OH stretches.

The presence of the sharp peak at 3680  $\text{cm}^{-1}$  indicates the existence of free OH bonds of water at the quartz-OTS-water interface, with the H atom pointing toward the solid wall. Hydrophobicity is therefore characterized by the lack of binding interactions between the protruding OH bond and the surface. In this respect, the air-water interface is also hydrophobic. Such a structure of water at a hydrophobic surface can be understood physically as follows: Water molecules are stabilized by tetrahedral bonding to their neighbors in the bulk. This arrangement is not possible for the surface water molecules, so a fraction of these hydrogen bonds must be broken. To minimize the surface free energy, the total number of hydrogen bonds each surface water molecule possesses should still be maximized. That condition can be satisfied if the surface water layer assumes roughly the structure of a hexagonal lattice, with the surface terminated by dangling OH bonds. In addition, the two OH bonds of a water molecule should have equal probabilities of orienting along any of the four tetrahedral bonding directions in order to avoid an overall dipole orientation of water molecules in the structure. This condition then leads to a configuration with about one dangling OH bond per four water molecules in the surface layer. This value was indeed roughly what we found at the air-water interface. The same is likely to be true for the quartz-OTS-water interface and is supported by the fact that the relative strength of the free OH peak (corrected by Fresnel factors) was nearly the same in the spectrum of Fig. 1A as in that of Fig. 1B. We also used an independent method to evaluate the surface density of free OH bonds at the air-water interface. We found that the free OH peak in the SFG spectrum could be completely suppressed by dissolving methanol ( $11 \pm 2\%$  in volume concentration) into the bulk water. The corresponding surface density of methanol in this case is  $2.5 \times 10^{14} \text{ cm}^{-2}$ , as deduced from the result of surface tension measurement in (13). It seems reasonable to expect that each methanol molecule appearing at the air-water interface is hydrogen-bonded to the originally free OH bond. One then finds that the  $2.5 \times 10^{14} \text{ cm}^{-2}$  methanol molecules needed at the surface to suppress the free OH peak in the spectrum correspond to the situation in which 25% of the water molecules in a full monolayer originally have one of their OH bonds free.

The broad spectral features in the region from 3000 to 3500  $\text{cm}^{-1}$  are due to hydrogen-bonded OH stretching modes. The

peak at  $\sim 3200 \text{ cm}^{-1}$  is generally attributed to in-phase vibrations of the coupled, symmetric OH stretch mode of the tetrahedrally coordinated water molecules (14) (the two H ends of the molecules are hydrogen-bonded to the neighboring molecules with equal strength). This peak dominates in the quartz-ice spectrum shown in Fig. 1D and is an indication of bond ordering (or ice-like structure) in the water molecular arrangement. The assignment of the peak at  $\sim 3400 \text{ cm}^{-1}$  is still somewhat controversial. Some researchers assign it to the symmetric stretch mode of asymmetrically bonded water molecules (molecules with one H strongly hydrogen-bonded and the other H weakly bonded to neighboring molecules) (14). Others assign it to molecules with bifurcated hydrogen bonds (15). In any case, this peak represents bond disordering in the water molecular arrangement. As seen in Fig. 1A, the spectrum of the water-hydrophobic solid interface in the bonded OH region is dominated by the peak at  $\sim 3200 \text{ cm}^{-1}$ , with only a weak shoulder at  $3400 \text{ cm}^{-1}$ . It closely resembles the spectrum of the quartz-ice interface (Fig. 1D) and therefore indicates that water molecules at this hydrophobic interface are well bond-ordered. This result is in fair agreement with the prediction of a recent molecular dynamics calculation (6). The result can again be understood from the physical consideration that the total number of hydrogen bonds should be maximized. As mentioned above, this condition is satisfied when the molecules form an ice-like structure, with the surface terminated by dangling OH bonds. At the water-hydrophobic solid interface, the rigid wall forces the surface water molecules into the more orderly ice-like structure because of the physical restriction involved in packing molecules against the wall.

The air-water interface, with about the same number of dangling OH bonds, is expected to follow roughly the same model. The difference is in the rigidity of the interface. The nonrigid air-water interface prevents the surface water molecules from being highly bond-ordered. This is reflected in the appearance of the pronounced bond-

disordered peak at  $3400 \text{ cm}^{-1}$  in the spectrum in Fig. 1B. The same should be expected for a hydrophobic oil-water interface. It was indeed found to be the case with the hexane-water interface (obtained by spreading a thin layer of hexane on water). The SFG spectrum of the hexane-water interface (Fig. 1C) is similar to that of the air-water interface (Fig. 1B). The existing molecular dynamics study does suggest that the hydrophobic liquid-water interface is rough, but it fails to predict a preferred orientation of water molecules at the interface (7).

We have also studied the interface between water and a partly wettable solid substrate. The latter was prepared by adsorbing on a fused quartz substrate a monolayer of DMOAP [*N,N*-dimethyl-*N*-octadecyl-3-aminopropyltrimethoxysilylchloride,  $\text{CH}_3(\text{CH}_2)_{17}(\text{Me})_2\text{N}^+(\text{CH}_2)_3\text{Si}(\text{OMe})_3\text{Cl}^-$ ] (16). The head group of DMOAP is much larger than the cross section of the hydrocarbon chain, so that our quartz surface was covered with a layer of loosely packed hydrocarbon chains with a high density of kink defects (8, 17). The SFG spectrum for the air-DMOAP-quartz interface is shown in Fig. 2A. The sharp peaks at  $2850 \text{ cm}^{-1}$  can be attributed to the  $\text{CH}_2$  symmetric stretch mode, which becomes observable when a sufficient number of kink defects appear on the alkyl chains to break the symmetry. The peak at  $2940 \text{ cm}^{-1}$  is mainly from the  $\text{CH}_2$  asymmetric stretch mode, with perhaps some contribution from the Fermi resonance peak of the  $\text{CH}_3$  stretch mode. The broad but relatively weak spectral features from 3000 to  $3600 \text{ cm}^{-1}$  are presumably from water molecules adsorbed on the DMOAP-covered surface from air. The SFG spectrum for the quartz-DMOAP-water interface (Fig. 2B) is very different. The disappearance of the  $\text{CH}_2$  peaks indicates that the alkyl chains must have been straightened considerably by interacting with surrounding water molecules. The enhanced spectral intensity of the hydrogen-bonded OH stretching modes results from the field-oriented surface water molecules: The ionized head groups of DMOAP adsorbed on the surface establish a strong surface field, much as in the case of the quartz-water interface at high pH (10), and

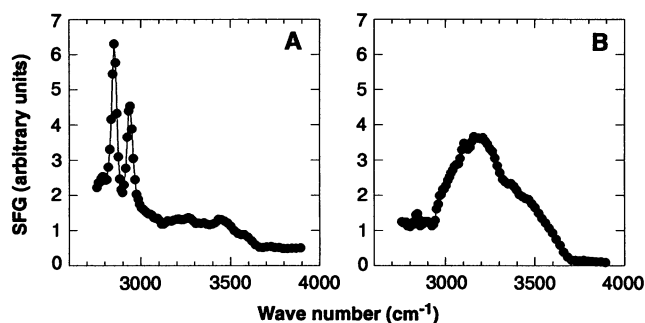


**Fig. 2.** SFG spectra from (A) the air-DMOAP-quartz interface and (B) the quartz-DMOAP-water interface. The polarization combination is the same as that in Fig. 1.

this strong field can orient several layers of water molecules at the interface to yield the enhanced spectrum. No free OH peak is discernible. These observations indicate that water molecules must have surrounded the hydrophobic chains. The partly wettable surface then corresponds to a situation in which the bulk water contacts a surface covered partly by water (hydrophilic) and partly by hydrocarbon (hydrophobic).

We can now describe a hydrophobic interface at the molecular level as follows: The surface water molecules do not interact strongly with the opposing surface. They form a hydrogen-bonding network, with dangling OH bonds on one-fourth of them. This large number of dangling OH bonds gives rise to a large interfacial surface energy (18). In this respect, air or vapor (or gas) is hydrophobic and also forms a hydrophobic interface with water. The hydrogen-bonding network of the surface layer can be more or less ordered, depending on the opposing hydrophobic surface. For a solid surface, the restriction of packing surface water molecules against the rigid wall forces the molecular arrangement into a more ordered, ice-like structure. For air-water and oil-water interfaces, no such packing restriction exists, and the interface water layer is less ordered. In the case of a partly wettable substrate prepared by surface coverage with a monolayer of loosely packed alkyl chains, water molecules appear to penetrate into the surfactant layer and induce a straightening of the alkyl chains.

## REFERENCES AND NOTES

1. W. Zisman, *Adv. Chem. Ser.* **43**, 1 (1964); G. M. Whitesides and P. Z. Laibinis, *Langmuir* **6**, 87 (1990).
2. J. N. Israelachvili, *Intermolecular and Surface Forces* (Academic Press, London, 1989), chaps. 15–17.
3. R. Pethig, *Annu. Rev. Phys. Chem.* **43**, 177 (1992); C. Tanford, *The Hydrophobic Effect* (Wiley, New York, ed. 2, 1980), pp. 1–35.
4. C. Chothia and J. Janin, *Nature* **256**, 705 (1975); J. Janin and C. Chothia, *Biochemistry* **17**, 2943 (1978).
5. S. L. Carnie and G. M. Torrie, *Adv. Chem. Phys.* **56**, 141 (1984); K. Raghavan, K. Foster, M. Berkowitz, *Chem. Phys. Lett.* **177**, 426 (1991); D. A. Rose and I. Benjamin, *J. Chem. Phys.* **98**, 2283 (1993), and references therein.
6. C. Y. Lee, J. A. McCammon, R. J. Rossby, *J. Chem. Phys.* **80**, 4448 (1984).
7. I. L. Carpenter and W. J. Hehre, *J. Phys. Chem.* **94**, 531 (1990).
8. P. Guyot-Sionnest, J. H. Hunt, Y. R. Shen, *Phys. Rev. Lett.* **59**, 1597 (1988); R. Superfine, J. H. Huang, Y. R. Shen, *ibid.* **66**, 8 (1991).
9. Q. Du, R. Superfine, E. Freysz, Y. R. Shen, *ibid.* **70**, 2313 (1993).
10. Q. Du, E. Freysz, Y. R. Shen, *ibid.* **72**, 238 (1994).
11. A picosecond passive-active mode-locked yttrium-aluminum-garnet-Nd laser system produced 0.5-mJ visible pulses at 0.532  $\mu\text{m}$  and 0.2-mJ infrared pulses that were tunable from 2700 to 3900  $\text{cm}^{-1}$ . Both the visible and the infrared pulses were incident at angles around 47° from the hydrophobic side and were overlapped at the water interface to be probed.

- Ultrapure water [resistivity greater than 18 megohm-cm, obtained from a Millipore (Bedford, MA) filtration system] and a Teflon cell were used in the experiment.
12. J. Sagiv, *J. Am. Chem. Soc.* **102**, 92 (1980).
  13. J. J. Kipling, *J. Colloid Sci.* **18**, 502 (1963).
  14. J. R. Scherer, in *Advances in Infrared and Raman Spectroscopy*, R. J. H. Clark and R. E. Hester, Eds. (Heyden, Philadelphia, 1978), vol. 5, pp. 149–216.
  15. P. A. Gignere, *J. Raman Spectros.* **15**, 354 (1984).
  16. The sample was made according to the method of F. J. Kahn [*Appl. Phys. Lett.* **22**, 386 (1973)]; the advancing and receding contact angles of it were 95° and 60°, respectively.
  17. J. Y. Huang, R. Superfine, Y. R. Shen, *Phys. Rev. A* **42**, 3660 (1990).

18. From the average hydrogen bonding energy of 15.5  $\text{kJ mol}^{-1}$  for water, the increase in surface energy resulting from the appearance of dangling OH bonds on 25% of the surface water molecules is 67  $\text{mN m}^{-1}$ . The experimental values of surface tension and surface energy for an air-water interface at 20°C are 72 and 116  $\text{mN m}^{-1}$ , respectively [M. A. Floriano and C. A. Angell, *J. Phys. Chem.* **94**, 4199 (1990)].
19. We thank R. Superfine for his involvement at the beginning of this project. This work was supported by the director of the Office of Energy Research, Office of Basic Energy Sciences, Materials Sciences Division, U.S. Department of Energy, under contract DE-AC03-76SF00098.

28 December 1993; accepted 29 March 1994

# A Crested Theropod Dinosaur from Antarctica

William R. Hammer\* and William J. Hickerson

Jurassic fossil vertebrates collected from the Falla Formation in the Central Transantarctic Mountains included a partial skull and postcranial elements of a crested theropod, *Cryolophosaurus ellioti* gen. nov. sp. nov. The theropod bears some resemblance to the large tetanurans of the Middle to Late Jurassic but also has primitive ceratosaurian features. Elements from a prosauropod, teeth from scavenging theropods, a pterosaur humerus, and a tritylodont molar were also recovered. The presence of this fauna suggests that a mild climate existed at high paleolatitude in this area of Gondwana during the Early Jurassic.

A number of high-latitude Cretaceous dinosaurs have been found recently, which indicates that these animals were not restricted to tropical or subtropical areas (1, 2). Few high-latitude dinosaurs are known from the Jurassic, particularly from the early part of the period before the breakup of Pangea. We describe an assemblage of Early Jurassic tetrapods collected from Mount Kirkpatrick near the Beardmore Glacier in the Transantarctic Mountains, Antarctica, approximately 650 km from the geographic South Pole (Fig. 1). The existence of this assemblage, which is similar to Early Jurassic assemblages from other continents, indicates that there were no geographic or climatic barriers to prevent dinosaurs from populating high southern latitudes during the Jurassic.

The fossils occur in a tuffaceous siltstone high in the Falla Formation (3) at an elevation of over 4000 m. All but three of the numerous bones collected were concentrated within a single meter stratigraphically and 5 m laterally. At least four dinosaurs (including a new theropod) and two non-dinosaurian taxa make up the fauna. The theropod is one of only a few reasonably complete Jurassic carnivorous dinosaurs known from any of the Gondwana continents; thus, it provides important information about the earlier stages of evolu-

tion of the large theropods. The specimen has a mixture of primitive and derived features and shows that Early Jurassic large theropods had diverged considerably from their Triassic ancestors.

The fossils include a partial skull with articulated mandibles and postcranial elements of a large crested theropod, *Cryolophosaurus ellioti* gen. nov. sp. nov. (4). The deep narrow skull is approximately 65 cm long. The nasals extend posteriorly as high ridges that join with a large furrowed lacrimal crest (Figs. 2 and 3, A and B). Above the orbits, the crest runs approximately perpendicular to the length of the skull and curves anteriorly as it rises. Although the top of the crest is broken, its furrowed

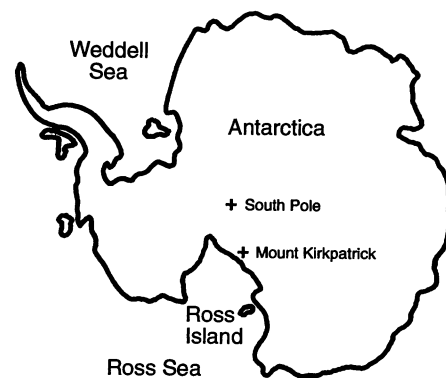


Fig. 1. Map showing location of Mount Kirkpatrick where Antarctic Jurassic fauna was discovered.

Department of Geology, Augustana College, Rock Island, IL 61201, USA.

\*To whom correspondence should be addressed.